ELECTRON BEAM DIAGNOSTIC SYSTEM FOR THE JAPANESE XFEL, SACLA

H. Maesaka#, H. Ego, C. Kondo, T. Ohshima, H. Tomizawa, Y. Otake,
RIKEN SPring-8 Center, Kouto, Sayo-cho, Sayo-gun, Hyogo, Japan
S. Matsubara , T. Matsumoto, K. Yanagida,
Japan Synchrotron Radiation Research Institute, Kouto, Sayo-cho, Sayo-gun, Hyogo, Japan

Abstract

We present the design and performance of the beam diagnostic instruments for the Japanese x-ray free electron laser (XFEL) facility, SACLA. XFEL radiation is generated by self-amplified spontaneous emission (SASE) process in SACLA, which requires a highly brilliant electron beam with a normalized emittance of less than 1 mm mrad and a peak current of more than 3 kA. To achieve this high peak current, 1 A beam with 1 ns duration from a thermionic electron gun is compressed down to 30 fs by means of a multi-stage bunch compression system. Therefore, the beam diagnostic system for SACLA was designed for the measurements of the emittance and bunch length at each compression stage. We developed a high-resolution transverse profile monitor and a temporal bunch structure measurement system with a C-band rf deflecting cavity etc. In addition, the precise overlapping between an electron beam and radiated x-rays in an undulator section is necessary to ensure XFEL interaction. Therefore, we employed a C-band sub-μm resolution rf cavity BPM to fulfill the demanded accuracy of 4 μm. All the performances of our developed beam monitors reached the demanded resolutions. By using these beam diagnostic instruments, the first x-ray lasing at a wavelength of 0.12 nm was achieved and SACLA has been stably operated for user experiments since March, 2012 in the wavelength region from 0.08 nm to 0.25 nm.

INTRODUCTION

The x-ray free electron laser (XFEL) facility, SACLA (SPring-8 Angstrom Compact Free Electron LAser) [1], was successfully commissioned and the first x-ray lasing was observed in June, 2011 at an x-ray wavelength of 0.12 nm. SACLA has been stably operated for various user experiments since March, 2012 in the wavelength region from 0.08 nm to 0.25 nm. In SACLA, XFEL radiation is generated by a self-amplified spontaneous emission (SASE) process. The SASE process in the x-ray region requires a high peak current of more than 3 kA and a small normalized emittance of less than 1 mm mrad [2].

To achieve these requirements, we designed and constructed a low-emittance injector, an 8 GeV C-band accelerator and a short-period in-vacuum undulator beamline, as shown in Fig. 1. An electron beam is generated by a thermionic electron gun with a CeB_6 cathode. The normalized emittance of the electron beam is 0.6 mm mrad, the initial current is 1 A and its pulse width is 1 ns (FWHM) formed from 3 μs (FWHM) by a high-voltage chopper. The beam is accelerated to 8 GeV by the following series of rf accelerator cavities: 238 MHz pre-buncher, 476 MHz booster, L-band (1428 MHz), S-band (2856 MHz) and C-band (5712 MHz) accelerators. In the meantime, the bunch length is shortened from 1 ns to 30 fs by using a velocity bunching process through the sub-harmonic acceleration cavities and a bunch compression process by means of three magnetic chicanes. The peak current is finally boosted up to 3 kA without substantial emittance growth. The electron beam is then fed into in-vacuum undulators with a period of 18 mm and the maximum K-value of 2.2, and XFEL light is finally generated.

In order to maintain the high gain SASE process at an x-ray wavelength, we need to monitor a beam position, a transverse beam profile, beam arrival timing and a temporal bunch structure at each acceleration stage. The resolution of the beam-position monitor in the undulator section is required to be less than 1 μm so as to maintain the overlap between the electron beam and radiated x-rays within 4 μm precision [3]. The transverse beam profile should be measured with a spatial resolution of less than 10 μm in order to measure a normalized emittance less than 1 mm mrad. The required resolution of the temporal bunch structure measurement is 10 fs at a position after the full compression, since the bunch length becomes 30 fs. In addition, since the initial bunch length is 1 ns, temporal profile monitors with a wide time scale from 1 ns to 10 fs are demanded. Therefore, we developed

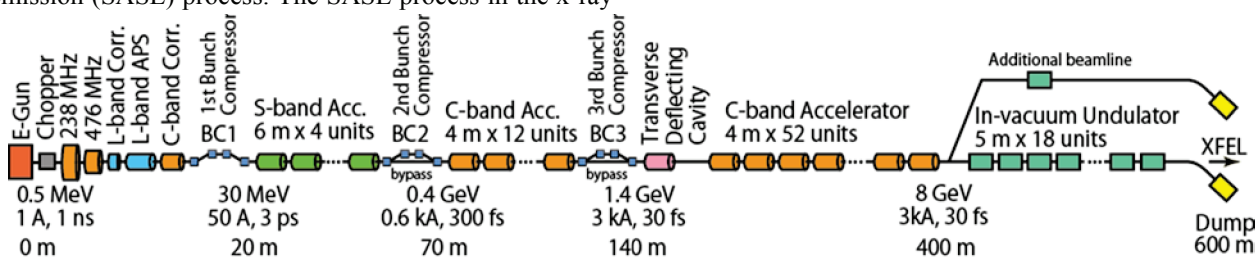

Figure 1: Schematic layout of SACLA.

maesaka@spring8.or.jp

ISBN 978-3-95450-119-9

bunch length monitors of several types.

In this paper, we describe the design and performance of each diagnostic instrument and demonstrate some results from the XFEL commissioning.

BEAM DIAGNOSTIC SYSTEM

The beam diagnostic instruments for SACLA can be classified into three categories: beam position monitor (BPM), transverse profile monitor and temporal profile monitor. In the following sections, the details of these three categories are described together with the experimental results of performance tests from the XFEL commissioning. In this section, we summarize the overview for each category. The number of monitors for each diagnostic instrument is listed in Table 1.

For the BPM, we employed rf cavity BPMs (RF-BPM) [4] for both the accelerator section and the undulator section in order to achieve sub-μm resolution. Although the accelerator section does not need such a high-resolution BPM, the same RF-BPM system is employed so as to reduce design and maintenance work. Only for the dispersive part of the three bunch compressors (BC1 – 3), multi-stripline BPMs [5] are used, since the beam width becomes wider than the aperture of the RF-BPM. In addition to the beam position measurement, RF-BPM has capability to detect the beam arrival timing [6]. Since some of the user experiments, such as a pump and probe experiment, require precise arrival timing, the timing information from the RF-BPM is provided for users.

For the transverse profile monitor, a screen monitor (SCM) [7] is employed. Optical transition radiation (OTR) or scintillation light from a target screen is focused by a lens system into a CCD camera, which records a beam. We employed a Desmarquest fluorescent screen for the low-energy beam part of the accelerator, a stainless steel foil for OTR or a YAG:Ce screen for a high-energy part. After full bunch compression, intense coherent OTR (C-OTR) was observed and the beam profile could not be obtained in this case. Therefore, we tried to mitigate the C-OTR effect [8].

For the temporal characteristic measurement of the electron beam, we designed several types of monitors, since the bunch length is compressed from 1 ns to 30 fs, which is too wide to measure the bunch length by one method. In the injector part, we use coherent transition radiation (CTR) from a screen monitor target and a fast differential current transformer (DCT) [9] in order to observe a bunch length of around 100 ps. The CTR monitor detects the intensity of the CTR, since the CTR intensity has a correlation with the bunch length. With the DCT, the bunch length is estimated from the pulse duration of the signal waveform. Coherent synchrotron radiation (CSR) monitors [10] are also utilized to measure the bunch length at the BCs. The intensity of CSR emitted from the fourth dipole magnet of each BC is detected, since the CSR intensity has bunch length information in the same way as the CTR monitor.

In order to directly measure the temporal beam profile, a streak camera and a C-band transverse rf deflector (RFDEF) [11] are employed. The streak camera detects the OTR from the metal foil. The streak camera system can measure the bunch length from sub-ps to 100 ps. The C-band RFDEF is installed downstream of BC3 in order to confirm the 30 fs bunch length after full bunch compression.

Table 1: List of beam diagnostic instruments and their numbers

	Number of Monitors
RF cavity BPM	57
Multi-stripline BPM	4
Screen Monitor	43
Differential Current Transformer	30
CTR monitor	5
CSR monitor	3
OTR screen for Streak Camera	3
Transverse RF Deflector	1

BEAM POSITION MONITOR

In this section, the design and performance of the RF-BPM and multi-stripline BPM (MS-BPM) are described. After the design overview of the RF-BPM, position resolution of the RF-BPM along the undulator beamline is analyzed and the orbit control for the beamline is also described. In addition, the resolution of the beam arrival timing and the trend of the timing during the SACLA operation are discussed. Finally, the technical details of the MS-BPM and the energy measurement performance are described.

RF Cavity Beam Position Monitor

A schematic drawing of the RF-BPM cavity is shown in Fig. 2. The beam position is detected by using a TM110 dipole mode cavity, which is tuned to be a resonant frequency of 4.76 GHz. In order to obtain both X and Y positions, the TM110 cavity has four coupling ports, two X ports and two Y ports. These four ports are symmetrically arranged so as to prevent field asymmetry. The signal amplitude from a TM110 cavity port can be written as

$$V = V_0 q x e^{j\omega t - t/T}$$

where V_0 is a proportionality constant, q is the beam charge, x is the beam position, ω is the resonant angular frequency and T is the time constant of the cavity. The amplitude of the beam-induced field in the TM110 cavity is proportional to the beam position. The sign of the beam position can be obtained from the rf phase of the signal.

The RF-BPM has additional TM010 monopole mode cavity with the same resonant frequency of 4.76 GHz. Since the TM010 mode is almost independent of the beam

ISBN 978-3-95450-119-9

position and the signal amplitude is only proportional to the beam charge. Furthermore, the phase of the TM010 mode signal is a normalization reference to the TM110 signal. By using both TM110 and TM010 signals, the beam position can be obtained.

The RF-BPM signal is processed by an IQ (In-phase and Quadrature) demodulator. The baseband signal from the IQ demodulator is recorded by a 12-bit or 16-bit VME A/D converter. The rf amplitude and phase of the TM110 and TM010 cavities are calculated from the baseband signal voltages at the specified timing and the beam position is calculated from these values.

Position Resolution Measurement

In order to confirm the sub-μm resolution demanded by the lasing condition in the undulator beamline, position resolutions of 20 RF-BPMs in the undulator section were measured [4]. The electron beam energy was 7 GeV and the bunch charge was 0.1 nC in this measurement. The beam position at a given RF-BPM was estimated from the other 19 RF-BPMs and the detected position was compared with the estimation. The estimated position was calculated by the least squares method. The details of analysis are described in Ref. [4].

Figure 3 shows an example of the correlation plot between the measured position and the estimated position. The estimation is almost the same as the measurement. We define the position resolution as the rms of the difference between the measured value and the estimated one. The position resolutions of 20 RF-BPM along the undulator section are plotted in Fig. 4. The resolution was less than 0.6 μm, which is sufficient for SACLA.

Steering Magnet Current Setting for Variable Gap Undulators Based on RF-BPM Data

In SACLA, variable-gap in-vacuum undulators are used for XFEL generation. Since the error magnetic field of the undulator depends on a gap width, a trajectory perturbed by the error field must be corrected by steering magnets in order to maintain the straightness of the beam orbit. For this purpose, each undulator is equipped with two steering magnets, one of which is placed at the entrance of the undulator and the other is at the exit.

The current setting of the steering magnet is determined by using RF-BPM data as a function of the undulator gap. Details of the analysis can be found in Ref. [12]. The orbit distortion was obtained from the RF- BPM data at each undulator gap. The current of the steering magnet as a function of the gap width is calculated from these data so as to reproduce the almost straight reference orbit.

The horizontal orbit reproducibility is shown in Fig. 5. In this data, the gap widths of all the undulators were changed at the same time and the steering magnet currents were set to appropriate values for individual gap widths. The beam orbit error from the straightness was within 10 μm for the entire gap variation region. By using the current setting data or the steering magnet, the XFEL can be generated with any K-value from 1.5 to 2.1

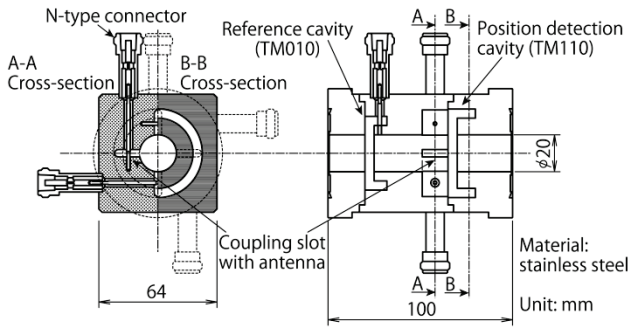

Figure 2: Drawing of the RF-BPM cavity.

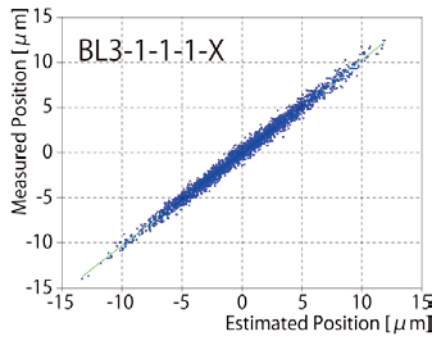

Figure 3: Scatter plot of the measured position of a BPM versus the estimated position from other BPMs.

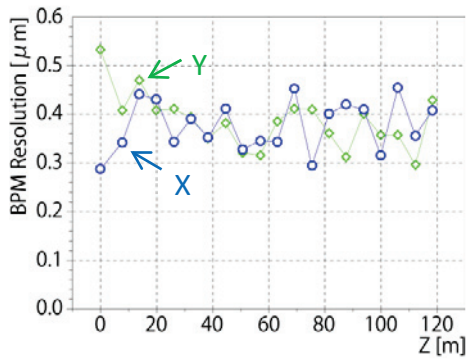

Figure 4: Position resolutions of 20 RF-BPMs along the undulator beamline.

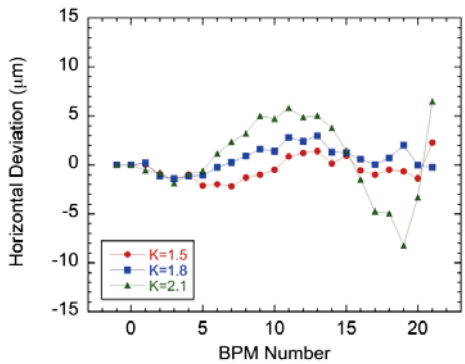

Figure 5: Reproducibility of the beam orbit after changing the undulator gap. The K values of 1.5, 1.8 and 2.1 correspond to the gap width of 5.2 mm, 4.4 mm and 3.7 mm, respectively.

ISBN 978-3-95450-119-9

Injection Orbit Stabilization for the Undulator Beamline

In order to constantly maintain the XFEL intensity, the beam orbit in the undulator beamline should be stabilized. In SACLA, an initial orbit drift is measured by two RF-BPMs upstream of the undulator beamline and the orbit is stabilized by a feedback control of two steering magnets upstream of these RF-BPMs. The period of the feedback control is a few seconds. A contour plot of the XFEL intensity as a function of these RF-BPM data is shown in Fig. 6. The XFEL intensity depends on the injection orbit. Therefore, the target point of the feedback control is set to the peak of the contour plot of the XFEL intensity. By using this control sequence, the XFEL intensity drift is sufficiently reduced.

Beam Arrival Time Measurement

As described previously, the beam arrival timing can be measured by the phase of the TM010 resonator of the RF-BPM. The resolution of the arrival timing was measured at the SCSS test accelerator by using the two neighboring RF-BPMs [6]. Figure 7 shows the distribution of the phase difference between the two TM010 cavities. The standard deviation is 0.0459 degree at 4760 MHz, corresponding to 27 fs. This value is $\sqrt{2}$ times larger than the timing resolution of each RF-BPM, if we assume the resolution of each RF-BPM is the same. Therefore, the arrival timing resolution is approximately 20 fs.

In order to estimate the long-term reliability of the arrival timing measurement, we analyzed a long-term variation of the beam arrival time by using the RF-BPM data [13]. Figure 8 shows a trend graph of the phase of the TM010 cavity of the RF-BPMs at the entrance and the exit of the undulator beamline. The distance from the entrance and the exit of the undulator line is about 110 m. The phase of 1 degree corresponds to 600 fs. The timing of the averaged data was varied about 600 fs pk-pk. This drift was caused by a parameter drift of the injector part of the accelerator. Nevertheless, the RF-BPMs themselves detected the beam arrival timing correctly, since the two graphs show a same tendency. Although a small difference can be seen, this difference is consistent with the thermal expansion of the optical fiber for the reference rf signal transmission due to ambient temperature drift.

Multi-stripline BPM

A schematic drawing of the MS-BPM used at the dispersive part of the bunch compressor is shown in Fig. 9. The cross-section of the beam aperture of the MS-BPM has dimensions of 70 (x) x 10 (y) mm^2. On each top and bottom surface, five stripline electrodes are arranged with a 10 mm interval. Since the vertical opening of the MS-BPM is 10 mm, most of the electric field from a single electron is confined to within 10 mm. Therefore, we can roughly obtain a horizontal beam profile with a resolution of about 10 mm. The horizontal beam position is calculated to be the center of mass of the charge

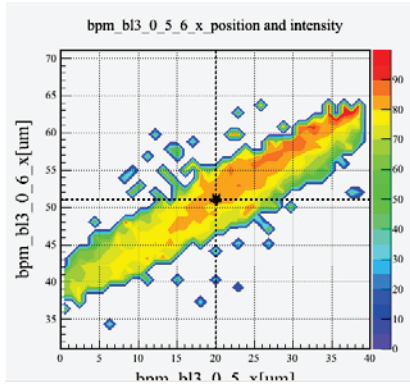

Figure 6: Contour plot of the XFEL intensity as a function of the injection beam orbit. The X and Y axes of this plot are the horizontal beam positions of the RF-BPM 7 m upstream from the first undulator and that of 1 m upstream of the first undulator, respectively. The Z-axis (color) shows the XFEL intensity.

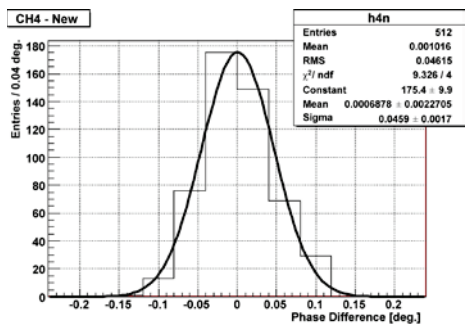

Figure 7: Phase difference between the reference cavities of the two adjacent RF-BPMs.

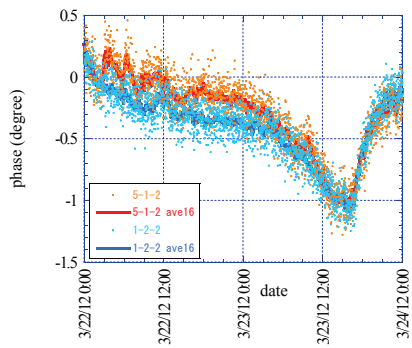

Figure 8: Trend graphs of the phases of the TM010 cavities of the RF-BPMs measured at the entrance (1-2-2) and the exit (5-1-2) of the undulator section for two days. The data of each beam shot is plotted by a dot and the 16-shot moving average is shown by a solid line.

distribution. The length of the stripline electrode is 160 mm, which corresponds to λ/4 of 476 MHz.

The signal from the MS-BPM is converted to a pulsed rf signal with a 476 MHz band-pass filter. Five rf signals are sequentially multiplexed into one channel by using a group delay of another band-pass filter. The multiplexed rf signal is detected by a 476 MHz IQ demodulators and the baseband signals generated with the detector are

ISBN 978-3-95450-119-9

recorded by a VME waveform digitizer board. The details of the MS-BPM system are described in Ref. [5].

We confirmed the position sensitivity of MS-BPM at the SCSS test accelerator [5]. The horizontal and vertical sensitivities were less than 0.1 mm and 0.01 mm. This horizontal sensitivity is sufficient for energy measurement at each bunch compressor, which is demanded to be less than 0.1%, since the dispersion of each bunch compressor is more than 100 mm. Since the beam energy at each bunch compressor is strongly correlated with a bunch compression ratio, the data from the MS-BPM is effectively used for beam tuning.

SPATIAL BEAM PROFILE MONITOR

In order to obtain a transverse beam profile, we use a screen monitor (SCM) with a fluorescent target and an optical transition radiation (OTR) target made of stainless steel. For a short bunch length beam of less than 100 fs, coherent OTR (C-OTR) was detected. Therefore, we tried to remove the C-OTR by using a YAG:Ce scintillation target and the spatial property of OTR. The emittance measurement result and the comparison of the position measurement result with the RF-BPM data to check the performance of the SCM are also described.

Screen Monitor

The SCM consists of a screen movement mechanism in vacuum and an imaging system [7]. The screen can be remotely inserted into the beam path with a pneumatic actuator. The radiation from the screen is focused by a custom-made lens system to a CCD camera, as shown in Fig. 10. The optical resolution of the lens system was confirmed to be 2 μm in case of the maximum magnification of x4.

Mitigation of Coherent OTR Effect

The SCM works well for a bunch length longer than 100 fs. However, intense C-OTR was observed from the stainless steel target when the bunch length was less than 100 fs and the beam profile image was no longer obtained. Therefore, we changed the target to the 0.1 mm-thick YAG:Ce in order to use scintillation light. Nevertheless, C-OTR was still observed from the YAG:Ce screen. We put an OTR mask in front of the lens, as illustrated in Fig. 11, since OTR is emitted in the forward direction with a radiation angle dependence of $1/\gamma$ [8]. After that, an appropriate beam profile image is obtained, as shown in Fig. 12.

Although the C-OTR mask method fairly works well, but non-negligible stray light of the C-OTR is often observed. Furthermore, even if the beam is scattered by the YAG:Ce screen, C-OTR is still generated at a mirror behind the YAG:Ce screen. In this case, it is difficult to remove C-OTR by using a mask. Therefore, we tried to use a perforated mirror to reduce the C-OTR effect [8]. A schematic drawing of the SCM with the perforated mirror is shown in Fig. 13. The C-OTR light generated at the YAG:Ce goes through the hole of the perforated mirror.

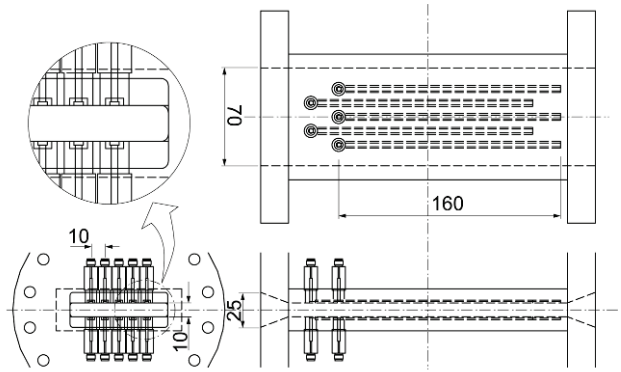

Figure 9: Schematic drawing of the multi-stripline BPM.

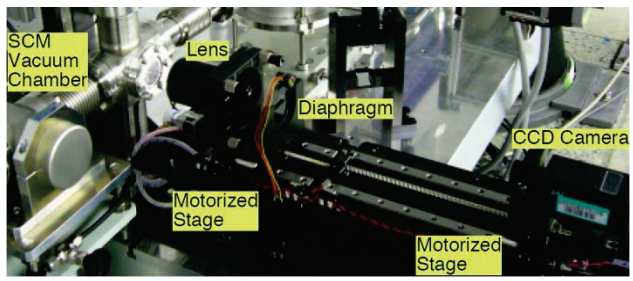

Figure 10: Photograph of the screen monitor.

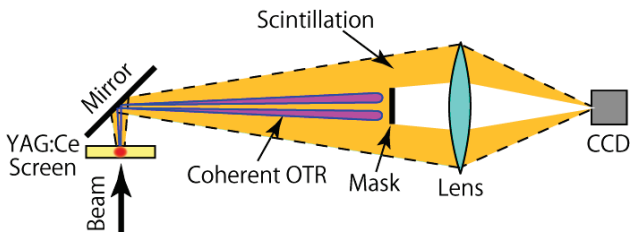

Figure 11: Setup of the screen monitor to mitigate C-OTR with a mask.

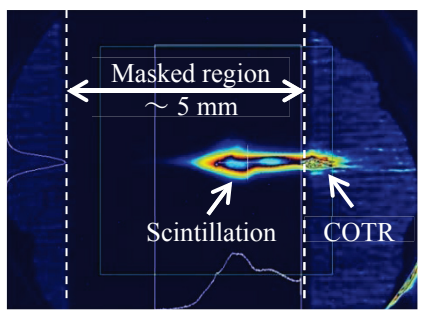

Figure 12: Beam profile image observed by the beam profile monitor with the YAG:Ce screen and OTR mask.

The electron beam also passed through the hole and hence the C-OTR is not generated at the mirror. Only the scintillation light from the YAG:Ce screen is reflected and the beam image can be obtained.

An example of the results is shown in Fig. 14. The hole diameter on the mirror is 3 mm in this measurement. The beam image was appropriately obtained and scattered light from the edge of the mirror hole can also be slightly seen. When the beam is moved near the edge of the hole by using a steering magnet, C-OTR radiation was

ISBN 978-3-95450-119-9

detected together with the scintillation beam image. Thus, C-OTR is sufficiently removed by this method.

Emittance Measurement

In order to generate intense XFEL radiation, the beam emittance should be as low as possible. Therefore, we measured the beam emittance at each stage of bunch compression. The emittance is measured by the quadrupole scan method [14]. We scanned the current value of the quadrupole magnet just upstream of a screen monitor and took the transverse beam size by using the screen monitor. The square of the beam size satisfies the following formula:

$$\sigma_x^2 = \beta\varepsilon\left(Ll_Q K + \alpha L/\beta - 1\right)^2 + \varepsilon L^2/\beta,$$

where σ_x is the rms beam size measured by the screen monitor, α and β are the Twiss parameters, ε is the emittance, L is the distance between the quadrupole magnet and the screen monitor, l_Q and K is the effective length and the K value of the quadrupole magnet, respectively. This formula is fitted to the data and the emittance and Twiss parameters are obtained.

One of the results is shown in Fig. 15. This data was taken after the bunch compression by BC3, and the screen monitor at about 15 m downstream from the exit of BC3. In this screen monitor, the YAG:Ce screen with the C-OTR mask was used. The data points were appropriately fitted by the analytical formula. The normalized emittance of this beam was 1.09 mm mrad, which was sufficient for XFEL. In this data, the minimum beam size was 30 μm rms and the profile of such a tiny beam can be appropriately obtained by the screen monitor with the YAG:Ce screen and C-OTR mask.

Comparison between Beam Positions Measured with RF-BPM and Screen Monitor

In order to confirm the validity of the measurements of the RF-BPM and the SCM, we compared the beam positions from the two monitors. We used a screen monitor in the undulator section and this screen monitor has the YAG:Ce screen with the C-OTR mask. The beam position from the SCM is calculated from the center of mass of the beam profile image and compared with the beam position data from the RF-BPM adjacent to the SCM. In order to change the beam profile, we scanned the beam energy from 3.8 GeV to 7.4 GeV, while the field strength of the quadrupole magnet was kept constant. Figure 16 shows the comparison between the RF-BPM and SCM position data. Even though the beam profile was changed, the beam positions measured with both the SCM and RF-BPM were consistent each other within the error of less than 10 μm (rms). Thus, the RF-BPM and the SCM with C-OTR mask are working well as expected.

TEMPORAL PROFILE MONITOR

A temporal beam profile is monitored with several methods depending on the bunch length. A fast differential current transformer (DCT) and a coherent transition radiation (CTR) monitor are used for the

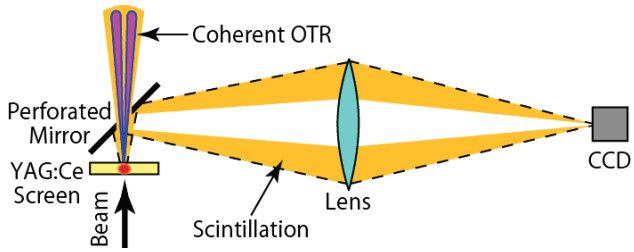

Figure 13: Setup of the profile monitor to mitigate C-OTR effect with the perforated mirror.

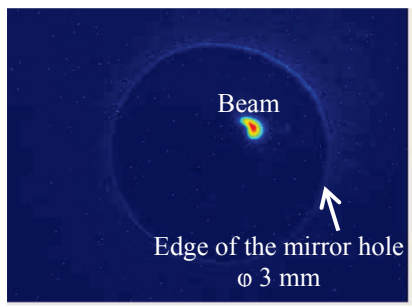

Figure 14: Beam profile image observed by the beam profile monitor with the YAG:Ce screen and perforated mirror.

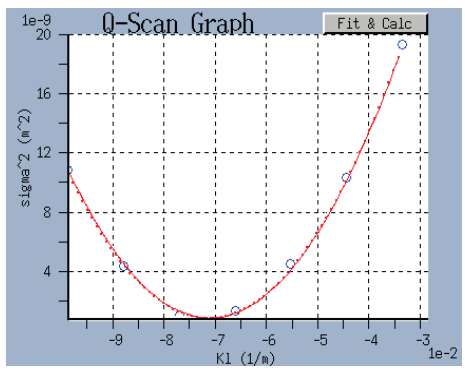

Figure 15: Emittance measurement result. The strength of the quadrupole magnet was scanned and the square of the beam size was plotted. This graph was fitted by the parabolic function and the emittance was calculated.

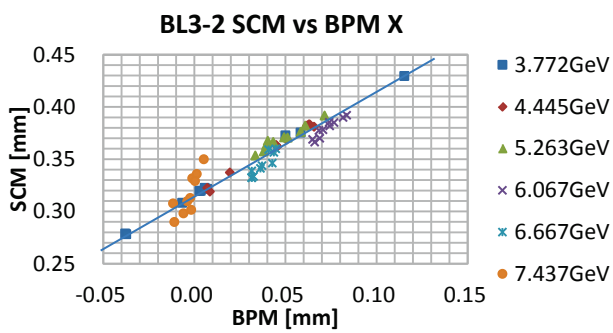

Figure 16: Correlation between the beam positions measured by an RF-BPM and a screen monitor. Even though beam energy was changed in order to vary the beam shape, the beam position was consistent each other.

ISBN 978-3-95450-119-9

injector part, where the bunch length is around 100 ps. For a non-destructive monitor of the bunch length at each bunch compressor, a coherent synchrotron radiation (CSR) monitor is utilized. For the direct detection of the temporal profile less than 10 ps, a streak camera and a C-band transverse rf deflector (RFDEF) are employed.

Fast Differential Current Transformer

We developed a high-speed DCT [9], as shown in Fig. 17. This DCT has four outputs: two are positive and the others are negative. By subtracting a negative signal from a positive one, we can remove any common-mode noise. A single-turn pickup coil and a high-frequency magnetic core (Finemet, Hitachi Metal, Ltd.) are used so as to achieve the short rise time of a DCT output pulse. The rise time of the raw signal was measured to be 200 ps. Therefore, this CT has a capability to measure the bunch length around 500 ps.

The bunch length of the injector part is measured with the two DCTs (CT-238 and CT-476), as shown in Fig. 18. The raw signals from these DCTs are taken by a 12 GHz band-width high-speed oscilloscope. An example of the raw signal waveform of CT-476 is shown in Fig. 19. In this data, an input rf power into the 238 MHz sub-harmonic buncher was changed and an rf phase was set to the bunching condition. The rf power for the other cavities were turned off. The pulse width and amplitude at CT-476 depend on the acceleration voltage and the bunch length is the shortest at an input power of 5.6 kW. Thus, we can obtain the bunching property of the injector part by using DCTs.

Coherent Transition Radiation Monitor

We use a CTR from a fluorescent screen in order to estimate the bunch length in the injector part, as shown in Fig. 20. Since the wavelength of the CTR is the same or longer than the bunch length, the bunch length can be obtained from the spectrum of the CTR. The CTR from the screen is reflected by a retractable mirror and detected by a CTR detector, as depicted in Fig. 21. The CTR detector has successively connected 5 rectangular waveguides and each waveguide has an antenna with a 50 GHz band-width rf detector. Since each rectangular waveguide has different cutoff frequency, we can obtain a rough spectrum of CTR. The cutoff frequencies of the 5 waveguides are 3, 6, 12, 24, 48 GHz.

Figure 22 shows a CTR intensity for each cutoff frequency as a function of the acceleration voltage of the 238 MHz sub-harmonic buncher. The CTR monitor used in this data is SCM-476 in Fig. 18. The CTR intensity has a peak around 175 kV, where the bunch length is the shortest at SCM-476. This is consistent with a 1D simulation result. Thus, the bunch length information was appropriately obtained with the CTR monitor.

Coherent Synchrotron Radiation Monitor

For a non-destructive bunch length monitor, a CSR monitor was developed [10]. A schematic view of the CSR monitor is illustrated in Fig. 23. CSR from the 4th dipole magnet of the bunch compressor chicane is reflected and extracted from the vacuum chamber. The CSR is then focused with a THz lens and detected with a pyro-electric detector.

Figure 24 shows a CSR intensity depending on the bunch length. The bunch length was varied by the rf

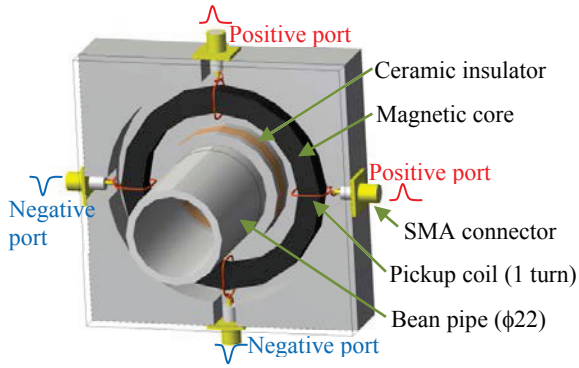

Figure 17: Schematic view of the differential CT.

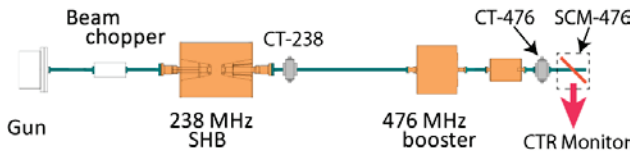

Figure 18: Schematic Drawing of the sub-harmonic buncher part.

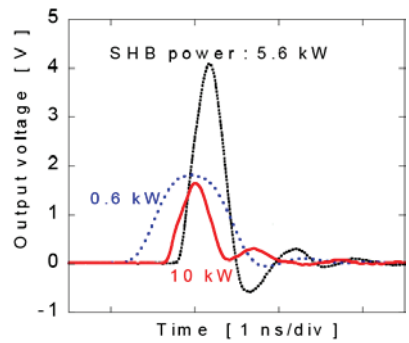

Figure 19: Waveforms of the DCT (CT-476). In this measurement, the acceleration voltage of the 238 MHz sub-harmonic buncher was changed.

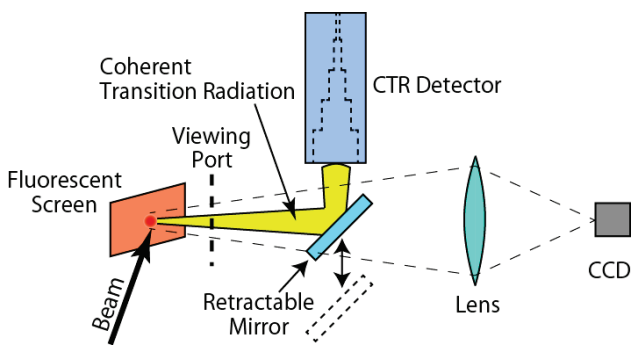

Figure 20: Schematic view of the CTR monitor attached to a screen monitor.

ISBN 978-3-95450-119-9

phase of the S-band accelerator upstream of BC2. In this data set, bunch lengths measured by the RFDEF system were 200 fs, 300 fs and 400 fs (FWHM) at -1, 0 and +1 degree, respectively. Here, the rf phase of 0 degree means the lasing condition of SACLA. The sensitivity of the CSR monitor to the S-band phase was 0.1 degree, which is sufficient for SACLA, and the linear response to the rf phase is suitable for the feedback control of the bunch length.

Streak Camera

In order to measure a bunch length from 300 fs to 100 ps, a streak camera system is used. OTR light emitted from a stainless-steel foil is transmitted to the klystron gallery and detected with a FESCA-200 streak camera [15], which is located downstream of BC2 or BC3. Figure 25 shows an example of a measured bunch length after BC2. The bunch length was 0.54 ps (FWHM) in this case. Thus, the streak camera system has capability to measure the bunch length less than 1 ps.

Transverse RF Deflecting Cavity

We use a C-band (5712 MHz) transverse rf deflecting cavity (RFDEF) [11] to measure the temporal bunch structure of the electron beam with a 30 fs bunch length after the full bunch compression. A schematic setup of the RFDEF system is shown in Fig. 26. The electron beam is pitched by a transverse deflecting rf field at a zero-crossing phase and the temporal structure is converted to a transverse profile. The transverse profile is observed by the SCM with the YAG:Ce screen with the OTR mask.

The rf mode excited in the RFDEF is HEM11 and the peak deflecting voltage of the RFDEF system is 60 MV. The drift space between the RFDEF and the SCM is approximately 10 m. In this case, the temporal sensitivity o RFDEF is approximately 50 fs/mm at a beam energy of 1.4 GeV, which was confirmed with measurement. Since the beam radius is about 0.1 mm, the temporal resolution is estimated to be 10 fs, which is limited by the emittance and orbital beta-function of the beam.

Peak-current and E-t Phase-space Measurement

Figure 27 shows a measured temporal bunch structure of a 1.4 GeV beam. The electron beam is vertically stretched by RFDEF. The bunch length of approximately 30 fs (FWHM) is appropriately obtained. The peak current is estimated to be more than 3 kA by the projected curve a graph of the beam image to the vertical axis.

Figure 28 shows an E-t phase space image of the electron beam. In this measurement, a quadrupole magnet at the dispersive part of BC3 was turned on and some dispersion was leaked at the SCM position. This E-t phase-space data is useful to obtain the bunch compression property.

SUMMARY

We developed and constructed high-resolution beam diagnostic instruments for the measurements of a beam position, a transverse profile and a temporal profile. A

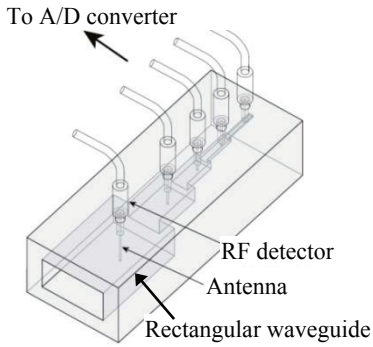

Figure 21: Schematic drawing of the CTR detector.

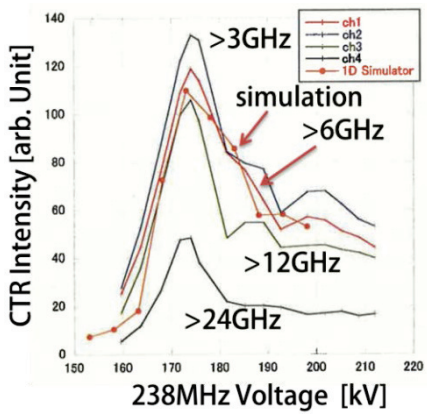

Figure 22: CTR intensity as a function of the acceleration voltage of the 238 MHz sub-harmonic buncher. Each solid line represents the CTR intensity for each cutoff frequency. The line with solid circles shows a 1D simulation result.

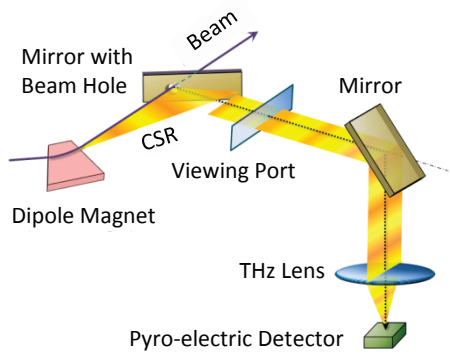

Figure 23: Schematic setup of the CSR monitor.

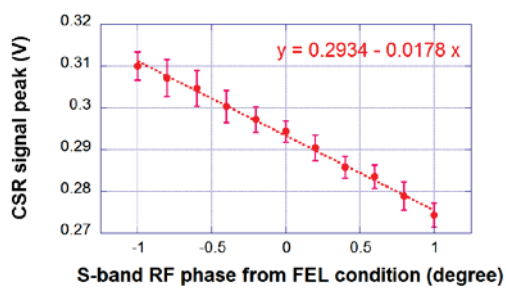

Figure 24: CSR intensity at BC2 as a function of the S-band acceleration rf phase. The origin of the horizontal axis is the phase at the XFEL lasing condition. Error bars represent the standard deviations of intensity fluctuations.

ISBN 978-3-95450-119-9

RF-BPM with a sub-μm resolution was successfully utilized for the XFEL commissioning of an undulator beamline. A MS-BPM has a sufficient energy sensitivity of less than 0.1% at each bunch compressor. A SCM also works well even under the condition of C-OTR irradiation. A spatial mitigation technique of C-OTR with a YAG:Ce screen was developed and the beam profile was appropriately obtained for a beam size of around 30 μm. A temporal bunch structure was monitored with a DCT and a CTR detector in an injector part and with a CSR detector at each bunch compressor. A sub-ps bunch length was directly measured with a streak camera system and a 30 fs bunch length was confirmed by using a C-band RFDEF. By using these beam diagnostic instruments, XFEL radiation in the wavelength region around 0.1 nm was successfully obtained and SACLA is stably operated for user experiments..

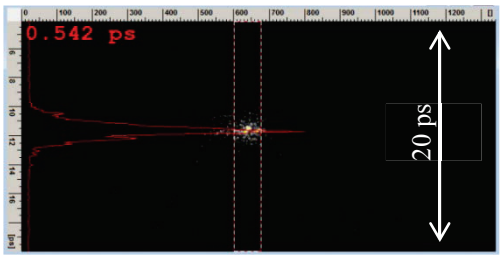

Figure 25: Example of a streak camera image. The temporal structure is stretched vertically. The full scale of the time range is 20 ps. The red line shows the projection of the image, which has the FWHM value of 0.54 ps.

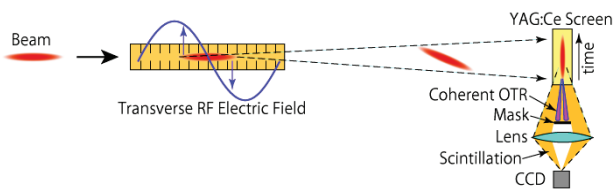

Figure 26: Schematic setup of the RFDEF system.

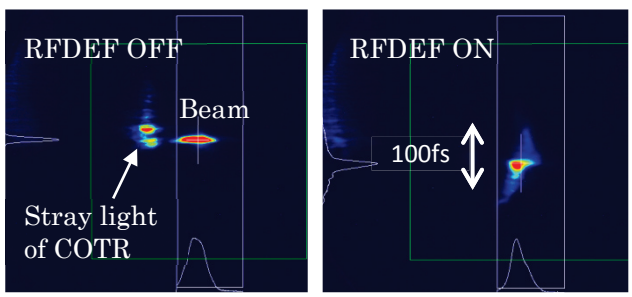

Figure 27: Beam profiles taken by the RFDEF system. The RFDEF is off in the left figure, and the RFDEF is on in the right one.

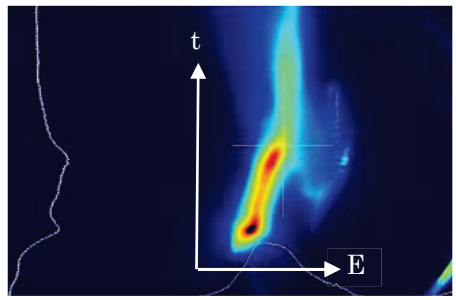

Figure 28: E-t phase-space image taken at the downstream of the RFDEF. A horizontal dispersion at the screen monitor was generated by a quadrupole magnet at the dispersive part of BC3.

REFERENCES

[1] T. Ishikawa, et al., Nature Photonics 6, 540-544 (2012).
[2] T. Shintake and T. Tanaka (eds.), "SCSS X-FEL Conceptual Design Report", RIKEN Harima Institute (2005).
[3] T. Tanaka, H. Kitamura and T. Shintake, Nucl. Instrum. Meth. A 528, 172 (2004).
[4] H. Maesaka, et al., Nucl. Instrum. Meth., doi: 10.1016/j.nima.2012.08.088, in press.
[5] H. Maesaka, et al., "Development of a Multi-Stripline Beam Position Monitor for a Wide Flat Beam of XFEL/SPring-8", Proceedings of IPAC'10, p. 954 (2010).
[6] H. Maesaka, et al., "Development of the RF Cavity BPM of XFEL/SPring-8", Proceedings of DIPAC'09, p. 56 (2009).
[7] K. Yanagida, et al., "Development of Screen Monitor with a Spatial Resolution of Ten Micro-Meters for XFEL/SPring-8", Proceedings of LINAC'08, p. 573 (2008).
[8] S. Matsubara, et al., "Improvement of Screen Monitor with Suppression of Coherent-OTR for SACLA", in these proceedings.
[9] S. Matsubara, et al., "Development of High-speed Differential Current Transformer Monitor", Proceedings of IPAC'11, p. 1227 (2011).
[10] C. Kondo, et al., "CSR Bunch Length Monitor for XFEL/ SPring-8–SACLA", Proceedings of IPAC'11, p. 1224 (2011).
[11] H. Ego, et al., "Transverse C-band Deflecting Structure for Longitudinal Phase Space Diagnostics in the XFEL/SPring-8 'SACLA'", Proceedings of IPAC'11, p. 1221 (2011).
[12] K. Togawa, et al., "Laser Wavelength Tuning by Variable-Gap Undulators in SACLA", Proceedings of FEL'12 (2012).
[13] T. Ohshima, et al., "Variation of Beam Arrival Timing at SACLA", Proceedings of FEL'12 (2012).
[14] S. Y. Lee, Accelerator Physics Second Edition, p. 62, World Scientific (2004).
[15] Hamamatsu Photonics K. K., http://www.hamamatsu.com/

ISBN 978-3-95450-119-9